

Design and Testing of a Prototype Pixellated CZT Detector and Shield for Hard X-Ray Astronomy

P. F. Bloser, J. E. Grindlay, T. Narita, and J. A. Jenkins

Harvard-Smithsonian Center for Astrophysics, 60 Garden St., Cambridge, MA 02138, USA

ABSTRACT

We report on the design and laboratory testing of a prototype imaging CZT detector intended for balloon flight testing in April 2000. The detector tests several key techniques needed for the construction of large-area CZT arrays, as required for proposed hard X-ray astronomy missions. Two $10\text{ mm} \times 10\text{ mm} \times 5\text{ mm}$ CZT detectors, each with a 4×4 array of 1.9 mm pixels on a 2.5 mm pitch, will be mounted in a “flip-chip” fashion on a printed circuit board carrier card; the detectors will be placed 0.3 mm apart in a tiled configuration such that the pixel pitch is preserved across both crystals. One detector is eV Products high-pressure Bridgman CZT, and the other is IMARAD horizontal Bridgman material. Both detectors are read out by a 32-channel VA-TA ASIC controlled by a PC/104 single-board computer. A passive shield/collimator surrounded by plastic scintillator surrounds the detectors on five sides and provides a $\sim 45^\circ$ field of view. The background spectrum recorded by this instrument will be compared to that measured by a single-element CZT detector ($10\text{ mm} \times 10\text{ mm} \times 2\text{ mm}$ high-pressure Bridgman material from eV Products) fitted with the same passive/plastic collimator but including an active BGO shield to the rear. This detector has been previously flown by us completely shielded by a passive cover. We describe preliminary laboratory results for the various systems, discuss initial background simulations, and describe our plans for balloon flight tests.

Keywords: CZT, background, shielding, balloon flights, hard X-ray astronomy, instrumentation

1. INTRODUCTION

Hard X-ray and gamma-ray detectors made of Cadmium Zinc Telluride (CZT) hold great promise for advancing the state of X-ray and gamma-ray astronomy instrumentation. The intrinsic energy resolution of semiconductor detectors is far greater than that of scintillators, and the use of pixel or strip electrode readouts allows far greater spatial resolution. The high density of CZT permits the photoelectric absorption of photons up to $\sim 500\text{ keV}$ with reasonable thicknesses ($\sim 5\text{ mm}$), and the high bandgap allows detectors to operate at room temperature (as opposed to germanium). It has been shown that the poor hole transport properties of CZT can be overcome by special readout electrode geometries that are sensitive to the motion of electrons only.¹ We have been pursuing a program to develop CZT detectors for astronomy applications, focusing specifically on the needs of a wide-field-of-view survey telescope operating in the hard X-ray band between 20 and 600 keV, such as the EXIST or EXIST-LITE concept.^{2,3}

In this paper we describe the CZT instruments we are preparing for a balloon flight in April 2000 as piggyback experiments on the Harvard EXITE2 payload. They are designed to test several of the key techniques that are needed to construct a large-area CZT detector plane, and to measure the CZT background at balloon altitudes with two different shielding configurations under consideration for a wide-field survey instrument.

2. TECHNICAL ISSUES IN CONSTRUCTING A HARD X-RAY SURVEY TELESCOPE

Many technical issues must be addressed before hard X-ray detectors suitable for astronomy can be constructed. The only practical method for imaging between 100 keV and 500 keV is the coded aperture technique,⁴ which requires a large area, position-sensitive detector. The wide field of view ($\sim 45^\circ$) of an individual survey telescope module^{2,3} together with the thick detectors needed for high energy response require relatively large pixels ($1.5\text{--}2.0\text{ mm}$) to avoid projection effects. Our work so far had thus focused on thick (5 mm) detectors with $1\text{--}2\text{ mm}$ pixels.⁵ At the same time, the resistivity of the material must be large to keep the noise due to leakage current from degrading the energy resolution, a problem made worse by large pixels. Thus we have also investigated the use of blocking contacts made from PIN junctions to reduce leakage current noise.⁶

Further author information: (Send correspondence to P. Bloser)
P.B.: E-mail: pbloser@cfa.harvard.edu

The sensitivity intended for EXIST (< 0.1 mCrab) requires several square meters of detector material. Presently the method of CZT crystal growth yielding the highest resistivity is the high-pressure Bridgman (HPB) technique. Although crystals grown in this manner have high resistivity, the process is costly since the yield of defect-free crystals any larger than $10\text{ mm} \times 10\text{ mm}$ is low. A major issue is then the construction of a large area detector by closely tiling thousands of small (1 cm^2) pixellated crystals with minimal dead space at at minimum cost, while incorporating the associated readout electronics. Recently IMARAD Imaging Systems has begun producing CZT using a modified horizontal Bridgman (HB) process⁷ which allows the growth of larger crystals ($40\text{ mm} \times 40\text{ mm}$) at higher yield and thus lower cost. The drawback is that the crystals have lower resistivity and thus higher leakage current. We are investigating IMARAD CZT detectors using various blocking contacts to reduce this leakage current noise.⁸

The main technical challenges are then creating a closely-tiled array out of small detector elements, reading out the thousands of pixels with the detectors and electronics in a compact package, and processing the signals from each channel. We have already begun working with IDE Corporation to test low-noise preamps and shaping amps in the form of application specific integrated circuits (ASICs) that are made as small as possible.^{5,6} The new CZT experiment described in detail in Section 4 begins to meet these challenges by placing two $10\text{ mm} \times 10\text{ mm} \times 5\text{ mm}$ CZT detectors with $\sim 2\text{ mm}$ pixels next to each other on a common carrier board in such a way that the pixel pitch is preserved. The pixels are mounted in “flip-chip” fashion such that the pixels are read out directly into traces on the carrier board and fed into a 32-channel ASIC controlled by a PC/104 single-board computer. One detector is eV Products HPB material, the other IMARAD HB material with blocking contacts, which allows comparative measures of in-flight background and performance under very similar conditions.

3. DESIGN OF THE BACKGROUND EXPERIMENT

Another critical issue for hard X-ray astronomy instrumentation is the background level in the detector system. Astronomical sources are faint in the hard X-ray range, and in coded aperture telescopes the noise per pixel is determined by the total counts in the entire detector. To achieve good signal-to-noise, therefore, the detector background must be kept to a minimum. Typically the background in balloon payloads is due to a combination of diffuse cosmic gamma-rays with gamma-ray photons and energetic particles resulting from cosmic ray interactions in the atmosphere and in the payload itself. Effective shielding requires a detailed knowledge of the physical processes that produce background counts in a given detector material. These processes must be determined by measurements and simulations. In May 1997 we flew a simple CZT background experiment consisting of a single-element CZT detector ($10\text{ mm} \times 10\text{ mm} \times 2\text{ mm}$) completely shielded with a passive Pb/Sn/Cu cup covering the front and sides and actively-shielded by a large BGO crystal to the rear.⁹ We found that the background rate in this CZT/BGO detector was reduced by a factor of ~ 6 when BGO triggers were used to veto events, and that the resulting “good event” rate ($9 \times 10^{-4}\text{ cts cm}^{-2}\text{ s}^{-1}\text{ keV}^{-1}$ at 100 keV) could be explained using GEANT simulations that included only gamma-rays leaking through the shields and produced in the surrounding passive material. Gamma-ray interactions alone could not, however, explain the six-times higher background that was rejected by the BGO, indicating that an internal activation component was also present that was effectively vetoed by the active shield. An additional goal in flying the new pixellated detectors is to make another measurement of the flight background spectrum with new shielding configurations, as well as to study its spatial distribution.

The large reduction in background achieved with the active shield in the CZT/BGO experiment led us at first to consider an active collimator of CsI combined with a rear CsI shield for the current imaging detector experiment. (BGO was not considered due to its cost.) However, detailed simulations have found that surrounding CZT detectors with thick material leads to increased background from activation, even if that material is active, and that a thin passive collimator with an active rear shield is preferable.¹⁰ We investigated the reduction in gamma-ray-generated background expected from an active collimator by performing two simple Monte-Carlo simulations using the CERN Program Library simulations package GEANT: a CZT detector at the bottom of a square well active collimator (45° field of view) made of 2.5 cm thick CsI, and a detector at the bottom of a square graded passive collimator made of 4 mm of Pb, 1 mm of Sn, and 1 mm of Cu. In both cases the CZT sat in front of a 2.5 cm thick CsI rear shield. Only the interactions of cosmic and atmospheric gamma-rays were considered (the passive collimator was assumed to be surrounded by plastic scintillator that vetoed gamma-rays produced locally from particle interactions). The spectra recorded per volume of CZT are shown in Figure 1. The CsI shield threshold was 50 keV . The spectrum recorded with the passive collimator is practically identical to that found with the active collimator at low energies, where aperture flux dominates, and is only $\sim 50\%$ higher at several hundred keV, suggesting that un-vetoed Compton scatters have

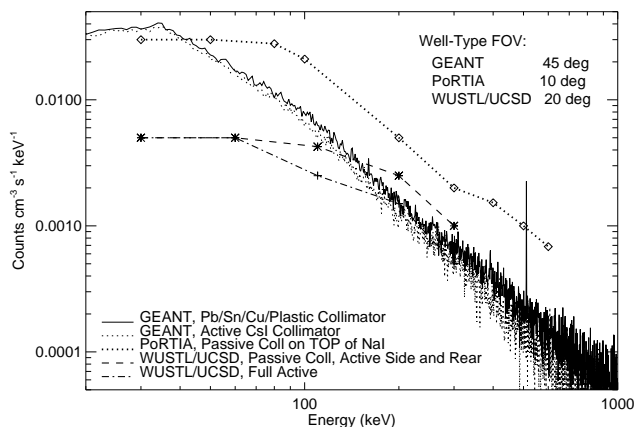


Figure 1. GEANT simulations of CZT detectors with active and passive/plastic collimators and an active rear shield, compared with previous measurements made using active rear shields and active or passive collimators. Spectra are plotted per volume to account for differing detector thicknesses. The fields of view are 45° for the GEANT simulations, 10° for PoRTIA, and 20° for the WUSTL/UCSD experiment.

only a modest effect on the overall background. This, together with the activation simulations mentioned above, indicates that an active collimator may not be optimal.

The factor of 6 reduction observed by the CZT/BGO experiment⁹ indicates that a large internal background is being generated in the CZT and vetoed by the BGO. This background is not due to shield-leakage gamma-rays, but presumably particle interactions such as prompt (n,γ) reactions. Thus we believe an active shield must be included in any CZT hard X-ray telescope. Though it has little effect on the gamma-ray component, would an active collimator further reduce the internal background component? In addition to our CZT/BGO balloon flight experiment, two other CZT background measurements at balloon altitudes have been performed using an active rear shield and active or passive collimation, and these have influenced the design of the present experiment.^{11,12,13} In 1995, a group from Goddard Space Flight Center flew the CZT experiment PoRTIA, containing a $25.4 \text{ mm} \times 25.4 \text{ mm} \times 1.9 \text{ mm}$ planar detector, in a number of configurations, including passively-collimated to a 10° field of view while sitting on top of a thick NaI crystal.¹¹ In 1998 groups from Washington University, St. Louis (WUSTL) and the University of California-San Diego (UCSD) flew a $12 \text{ mm} \times 12 \text{ mm} \times 2 \text{ mm}$ CZT detector with orthogonal strip electrodes in several different configurations, including one with active CsI shielding to the rear and sides with a passive collimator (20° field of view), and one in which the passive collimator was replaced with an active NaI collimator.^{12,13} In Figure 1 we have included the spectrum recorded by PoRTIA in the passive collimator/active rear shield, and the spectra measured by the WUSTL/UCSD detector in both the active shield/passive collimator and fully actively-shielded cases. All spectra are shown per volume to allow for differences in detector thickness. The PoRTIA background is ~ 3 times higher than the GEANT spectrum at all but the lowest energies, where the larger aperture flux from a 45° field of view dominates. It is not clear why the PoRTIA background is so much higher in this configuration, but it could be caused by local gamma-ray production in the passive collimator. The WUSTL/UCSD passively-collimated spectrum is slightly higher than the GEANT prediction above 150 keV while the actively-collimated spectrum agrees quite well with it. The active collimator reduces the background above 100 keV by a factor of 1.6–2. Below 100 keV the higher aperture flux assumed in the GEANT spectrum dominates. (The WUSTL/UCSD experiment also used a depth-sensing technique to reduce background at low energies,^{12,13} although this correction has not been applied to the spectra shown in Figure 1.) The WUSTL/UCSD background was 10 times higher when both the rear and collimating shields were turned off. These results indicate that active shielding, together with plastic particle shielding around passive material, is essential for achieving low backgrounds in CZT hard X-ray telescopes, and the simple GEANT simulations represent the “best-case” scenario of no internal background. The rear active shield does most of the work, however, and the additional reduction from the active collimator may not be worth the added complexity and the volume taken up by thick scintillator crystals, especially

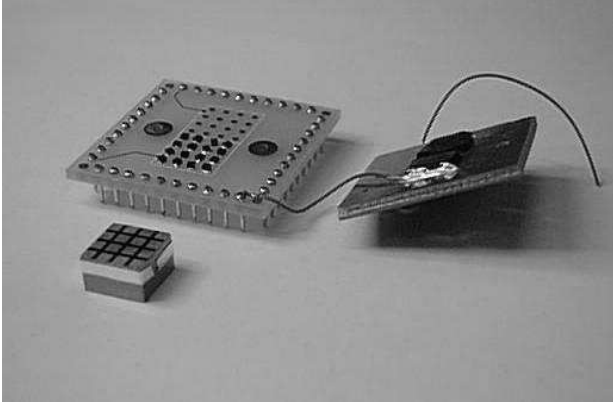


Figure 2. The IMARAD Au/In detector with the ceramic flip-chip carrier card. Conductive rubber pads connect the pixels to the pins via traces. The top cover delivers high voltage.

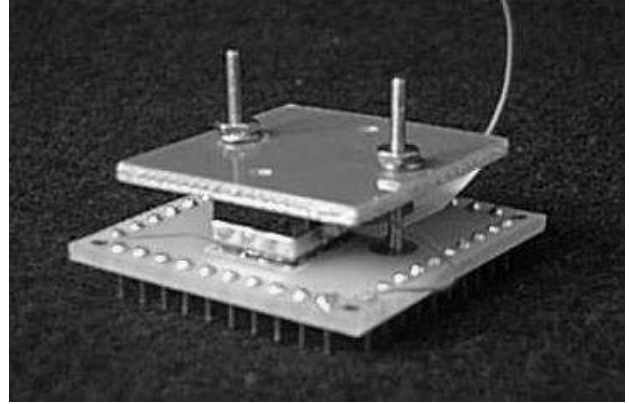


Figure 3. The assembled flip-chip CZT detector. The top cover (G10 material) holds the CZT between conductive rubber pads for readout and application of bias voltage.

if small segments of the CZT array need to be collimated individually. We therefore decided not to fly an active collimator with our imaging detectors.

To measure directly the importance of active shielding for our wide field of view survey telescope application, we have decided to fly two simultaneous background experiments on the next flight of the EXITE2 payload. The new pixellated, tiled detectors will be flown entirely passively-shielded, with a passive collimator (45° field of view) surrounded by plastic scintillator in the front and a passive/plastic rear shield in back. At the same time, the CZT/BGO detector will be flown again with the Pb/Sn/Cu cup in front replaced by a passive/plastic collimator identical to that on the pixellated CZT detector.

4. DESCRIPTION AND TESTING OF INSTRUMENT

The present experiment tests several of the key elements discussed in Section 2 that are needed for the development of coded-aperture CZT hard X-ray survey telescopes. Two thick CZT detectors ($10 \text{ mm} \times 10 \text{ mm} \times 5 \text{ mm}$) will be fabricated and flown in a tiled arrangement such that the pixel pitch is preserved across both detectors. This is the first important step in building up a large detector area out of small crystal elements. One of the detectors will be eV Products HPB material with gold contacts, similar to detectors we have tested at length.⁵ The second detector will be IMARAD HB material made with blocking contacts to reduce its leakage current and improve energy resolution.⁸ The exact choice of contact material for the IMARAD detector to be flown has yet to be determined, but for initial testing we have inserted the IMARAD Au/In detector we have tested previously in the lab.⁸ This detector was manufactured for us by IMARAD with indium pixels and a gold cathode that acts as a blocking contact. Both detectors will have 1.9 mm pixels on a 2.5 mm pitch (the IMARAD standard pixel size, for compatibility) and will thus operate within the “small-pixel regime.”¹ An outer guard ring will prevent surface leakage current around the edges. This requires making the outer pixels slightly smaller so that the two detectors may be tiled together while preserving pixel pitch.

The two pixellated detectors will be mounted in a “flip-chip” style on a specially-designed printed circuit board carrier card (made of standard FR-4 PCB material). Figure 2 shows the IMARAD Au/In detector together with the flip-chip carrier board and its cover. Gold pads are arranged to match each pixel and connect it to a pin via traces on the underside of the board. To allow us to remove and replace detectors easily, the electrical connection between the pixels and traces is made with conductive rubber pads held in place with a conductive epoxy made by TRA-CON, Inc. The top cover provides the negative high voltage to the cathode through another conductive rubber pad, which is connected by a wire to the bias voltage pin on the board. The cover is made of G10 material 0.06” thick and holds the detector in place between the rubber pads when it is screwed down. Figure 3 shows the assembled carrier board with the IMARAD Au/In detector in place. We have measured the transmission of the G10/rubber cover using the low energy lines of a ^{241}Am source. We find transmissions of 6% at 17 keV (Np line), 60% at 26.34 keV, and 90%

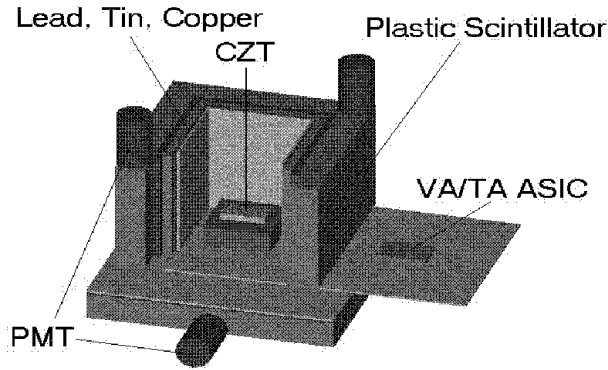


Figure 4. Layout of the tiled CZT experiment shielding, showing the detectors, VA-TA board, Pb/Sn/Cu collimator and rear shield, NE-102 plastic scintillator particle shield, and readout PMTs.

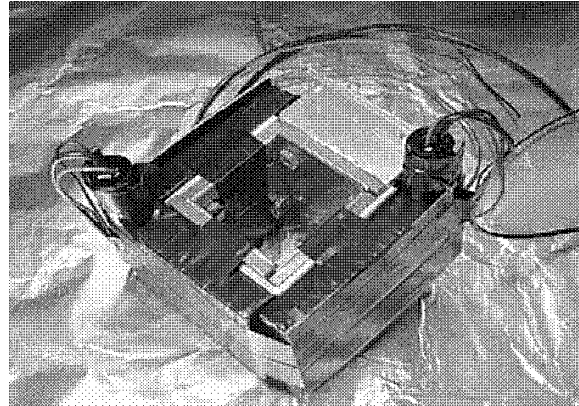


Figure 5. The assembled passive/plastic collimator. The Pb, Sn, and Cu slats are bolted on the inside of an aluminum frame, while the plastic shield takes the form of two L-shaped halves, each read out in the corner by a miniature PMT.

at 60 keV. The low energy absorption appears to be dominated by the G10, so to optimize the response down to 20 keV we will investigate alternative cover materials.

The two CZT detectors are read out by a 32-channel VA-TA ASIC manufactured by IDE Corp. The flip-chip carrier card plugs directly into a custom-made circuit board that contains the ASICs and associated bias resistors and decoupling capacitors. The VA-TA combination is attractive because it includes a self-trigger and MUX to output all 32 channels for each event. This will allow us to study the contribution of multiple-pixel events to the background and possibly to correct for the effects of charge-spreading between adjacent pixels.⁶ The expected count rate is ~ 1 count $\text{cm}^{-2} \text{s}^{-1}$ (see Figure 9), or ~ 2 counts s^{-1} from all 32 pixels together, easily low enough to record all channels for each event. The VA-TA ASICs are controlled by a data acquisition (DAQ) board supplied by IDE. We are in the process of writing software to control this DAQ board that will run on a PC/104 single-board computer flown alongside the detectors. This computer will record data into buffers and transfer them, along with housekeeping data, into the main EXITE2 data stream.

As described in Section 3, the two tiled flip-chip detectors will be surrounded by a passive/plastic collimator and rear shield. This is shown schematically in Figure 4. In order to keep the instrument weight down, the collimator only surrounds the CZT carrier board (~ 3 cm across), providing a 45° field of view. Since the current prototype VA-TA board is too large to fit within this space, it was necessary to have the collimator and rear shield physically separated. This required making the rear shield large enough to prevent the detectors from having a line of sight to the outside. Future designs will stipulate that the ASIC and its circuit board fit entirely within the footprint of the detector carrier card, so that they may be assembled vertically and fit within the main shielding.

Figure 5 shows the assembled passive/plastic collimator. The passive portion consists of 4.5 mm Pb, 1 mm Sn, and 1 mm Cu slats bolted within an aluminum support frame. Cosmic ray particles will interact in this dense material, generating gamma-ray photons. To prevent these locally-produced gamma-rays from producing background in the CZT, plastic shields surround the passive material to provide a veto pulse when charged particles pass through them. The shields are made of 0.5" thick NE-102 plastic scintillator joined with Bicon BC-600 optical cement into two L-shaped halves. The readout devices for such shields (and active gamma-ray shields as well) must be extremely compact if large-area arrays are to be built up of smaller detector/shield units. We have selected Hamamatsu R7400U miniature photomultiplier tubes (PMTs) as the readout devices for the plastic shields. These PMTs are only 1.5 cm across and 2.6 cm long, have far higher gain than photodiodes or avalanche photodiodes (APDs), and their gain is not temperature dependent as in APDs. One PMT is placed in the corner of each L to read out two sides of the plastic shield. We have tested this arrangement in the lab by setting up a muon telescope: two lab PMTs coupled to plastic scintillators were placed on either side of the shield. Only muons passing through all three scintillators generated a coincident signal, and using this coincidence we could identify pulses from particles interacting anywhere along the L. We found that particles passing through the shield on the opposite end from the readout PMT still

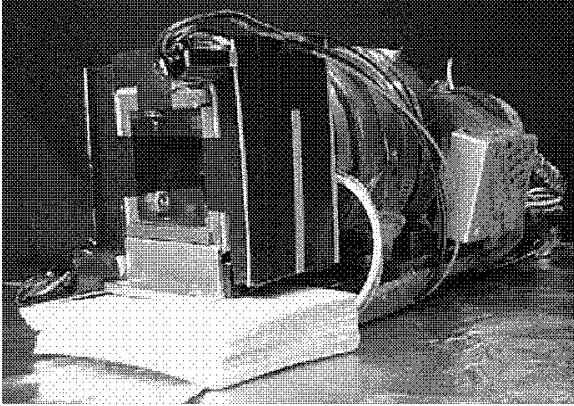


Figure 6. The passive/plastic collimator with the CZT/BGO detector in flight configuration. The BGO crystal is housed in the cylindrical container visible to the right of the collimator, and is read out by the large PMT behind that. This experiment will test the passive/plastic collimator and active rear shield configuration.

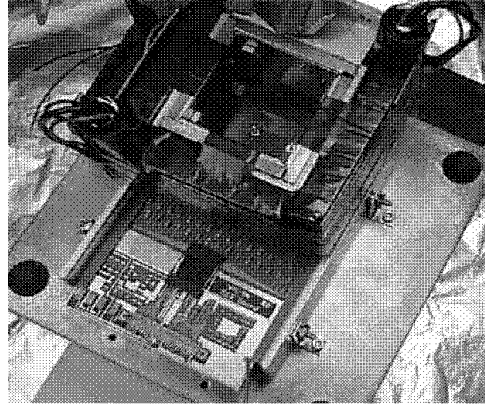


Figure 7. The passive/plastic collimator shown in the flight configuration with the tiled flip-chip detector assembly. The collimator surrounds the detector carrier board, which is plugged into the VA-TA board. The ASICs are mounted under the black rectangular cover to the lower left. The rear passive/plastic shield (not shown) will lie directly beneath the VA-TA board.

produce easily-measurable pulses, and so the two miniature PMTs are able to read out the entire volume of plastic. Pulses from the PMTs are fed into a coincidence-logic card that generates a veto pulse for coincident CZT and plastic triggers. The PC/104 computer will recognize this veto pulse and flag the event.

As described in Section 3, identical passive/plastic collimators will be flown with the old single-element CZT/BGO detector and the new pixellated tiled detectors. Figure 6 shows the passive/plastic collimator mounted in front of the CZT/BGO experiment. The CZT detector sits at the rear of the collimator and observes a 45° field of view. The BGO crystal is housed within the cylindrical container directly behind the CZT, and is read out by the large PMT at the rear. This setup will test the passive collimator/active rear shield configuration under consideration for future CZT telescopes.

Figure 7 shows the passive/plastic collimator in the flight configuration with the flip-chip detector assembly and VA-TA board. The detector is mounted in the carrier card, visible at the bottom of the collimator. As shown schematically in Figure 4, the VA-TA board extends out from under the collimator as presently constructed. The large passive/plastic shield will be mounted directly under the VA-TA board in flight. This setup will test the completely passively-shielded configuration for direct comparison with the actively-shielded case described above. The ASICs are mounted under the black rectangular cover visible beneath the collimator, and the connector that leads to the DAQ board is shown at the bottom of the figure.

Figure 8 shows the 4×4 array of “first light” ^{57}Co spectra from the 16 pixels of the IMARAD Au/In detector mounted on the flip-chip carrier card and read out through the VA-TA ASIC. Three channels are disconnected; it was found that these three conductive rubber pads had become detached during our initial attempts at mounting the detector. In addition, the channels in the top row are unusually noisy. Either a good connection was not made between the pixels and rubber pads, or these channels of the ASIC are picking up excess noise. In any case, the spectra in the lower left portion of the detector are comparable to those taken through more conventionally-mounted detectors,^{6,8} and so prove that our flip-chip mounting scheme is feasible.

5. DISCUSSION AND CONCLUSIONS

Both the CZT/BGO detector with its passive collimator and the pixellated flip-chip detectors with their passive/plastic shielding will be flown as piggyback experiments on the next flight of the EXITE2 hard X-ray telescope payload. This flight is scheduled to take place in April of 2000 from Ft. Sumner, NM. The expected gamma-ray contributions to the backgrounds of the CZT/BGO and flip-chip CZT detectors have been calculated using GEANT in the same manner as the spectra shown in Figure 1. These simulations then represent a “lower limit” to the total

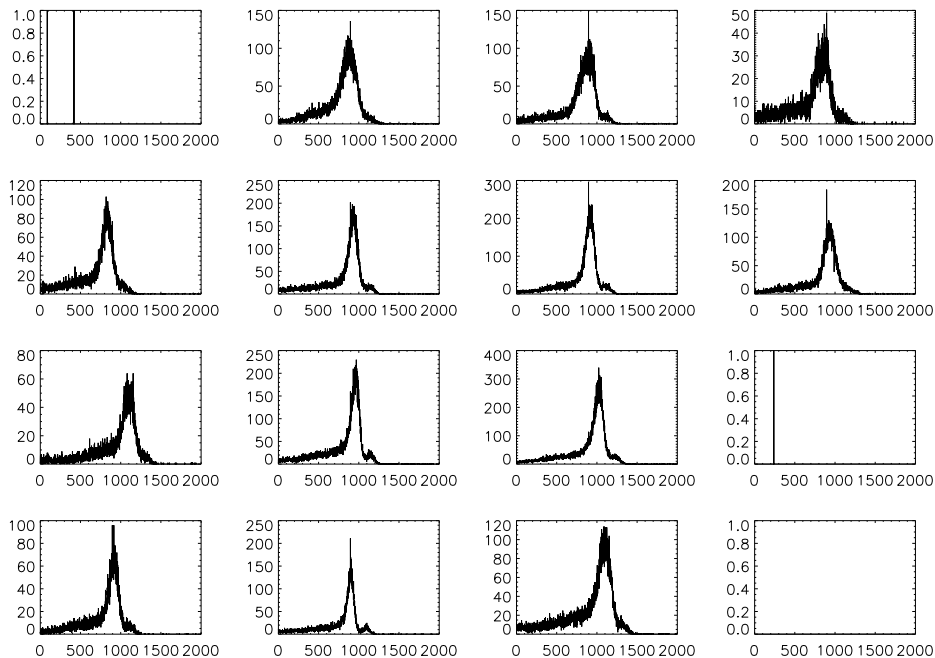


Figure 8. “First light” 4×4 array of ^{57}Co spectra taken with the IMARAD Au/In detector mounted on the flip-chip carrier card read out by the VA-TA ASIC. Three pixels were found to be disconnected because the conductive rubber pads had become detached. The pixels in the top row are unusually noisy, either due to bad contact with the pixels or noise in certain ASIC channels.

background expected. In Figure 9 we compare them to the PoRTIA and WUSTL/UCSD results as before. Here we plot the backgrounds per area, since the important quantity is the background counts within the area of a pixel. It is obvious that the thicker pixellated detectors in the passive/plastic shield can expect to record a higher background per pixel than would the thinner detectors in the other experiments. The pixellated detector background is higher by a factor of ~ 1.5 even at the lowest energies because these detectors are mounted slightly closer to the front of the collimator than is the CZT/BGO detector, giving them a slightly larger field of view and higher aperture flux. There is good agreement between the expected CZT/BGO background and the completely actively-shielded WUSTL/UCSD background at high energies. This might indicate that the WUSTL/UCSD experiment has successfully rejected most of the internal background and is recording mostly shield leakage photons. Whether the CZT/BGO background will really be this low will depend on the efficiency of the BGO active shield in rejecting prompt internal background. Our previous results⁹ indicate that the actual spectrum should lie within a factor of two of that plotted in Figure 9.

To compare the CZT/BGO and pixellated experiments without regard to detector thickness, we plot the GEANT spectra as a function of detector volume in Figure 10. The two backgrounds are in fairly close agreement. At low energies the background is dominated by aperture flux from the front. Both the thin CZT/BGO and thick pixellated detectors efficiently absorb these low energy photons, but the thin detector does so in a smaller total volume. Therefore the count rate in the thin detector appears higher when plotted per volume. At high energies the CZT/BGO background is slightly lower due to the rejection of Compton-scattered events. In reality, our results,⁹ together with those of the WUSTL/UCSD experiment,^{12,13} indicate that the background in the passive/plastic-shielded detectors will be 6–10 times higher than that in Figures 9 or 10. It will be of great value to measure how much higher it is, and to attempt to model the processes responsible for it.

As noted in Section 3, the WUSTL/UCSD experiment makes use of a depth-sensing technique to further lower the background below 100 keV by rejecting low energy events near the bottom of the detector.^{12,13} The method is based on the fact that the ratio of the cathode and pixel pulses for a given event should be proportional to the depth of the interaction. Such a technique would be even more useful in 5 mm thick detectors such as ours, and we

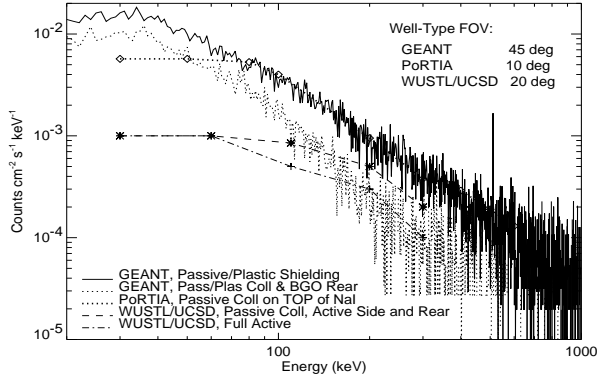


Figure 9. Expected gamma-ray backgrounds per area expected for the CZT/BGO detector with passive/plastic collimator and pixellated flip-chip detectors with passive/plastic shielding, as computed by GEANT. The PoRTIA and WUSTL/UCSD results are reproduced as in Figure 1. The thicker pixellated detectors record a higher background per area.

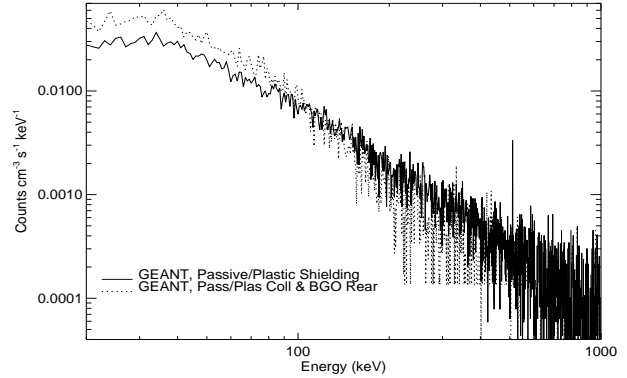


Figure 10. The GEANT spectra of Figure 9 plotted per detector volume. At low energies the thinner CZT/BGO detector has a greater fraction of its volume filled by aperture flux counts, and so the per volume count rate is higher. At high energies the CZT/BGO background is slightly lower, due to rejected Compton scatter events.

will implement it in our application by adding an extra channel to future ASICs to read out the cathode pulse.

To fully understand the background measurements we will make, it will be necessary to model the response of the CZT detectors themselves. We have already successfully simulated the simple response of the single-element CZT/BGO detector.⁹ Modeling a pixellated detector requires knowledge of the internal electric field and weighting potentials.¹ We have already developed electric field modeling tools based on the commercial software package ES4, and are now modeling the response of our tiled imaging detectors to laboratory X-ray sources. We will also attempt to include cosmic ray interactions and activation processes (e.g. $^{110}\text{Cd}(n,\gamma)$) in our background simulations in order to understand the internal background processes important in CZT.

ACKNOWLEDGMENTS

We thank F. Harrison and B. Matthews for providing the CZT/BGO detector for further flights. This work was supported in part by NASA grant NAG5-5103. P. Bloser acknowledges support from NASA GSRP grant NGT5-50020.

REFERENCES

1. H. Barrett, J. Eskin, and H. Barber, "Charge transport in arrays of semiconductor gamma-ray detectors," *Phys. Rev. Lett.* **75**, p. 156, 1995.
2. J. Grindlay, T. Prince, N. Gehrels, J. Tueller, C. Hailey, B. Ramsey, M. Weisskopf, P. Ubertini, and G. Skinner, "Energetic X-ray Imaging Survey Telescope (EXIST)," *Proc. SPIE* **2518**, p. 202, 1995.
3. J. Grindlay, "Balloon-borne hard x-ray imaging and future surveys," *Adv. Space Res.* **21**, p. 999, 1998.
4. E. Caroli, J. Stephen, G. DiCocco, L. Natalucci, and A. Spizzichino, "Coded aperture imaging in x- and gamma-ray astronomy," *Space Sci. Rev.* **45**, p. 349, 1987.
5. P. Bloser, T. Narita, J. Grindlay, and K. Shah, "Prototype imaging Cd-Zn-Te array detector," in *Semiconductors for Room-Temperature Radiation Detector Applications II*, R. James, T. Schlesinger, P. Siffert, M. Cuzin, M. Squillante, and W. Dusi, eds., *Proc. MRS* **487**, p. 153, 1998.
6. T. Narita, P. Bloser, J. Grindlay, R. Sudharsanan, C. Reiche, and C. Stenstrom, "Development of prototype pixellated PIN CdZnTe detectors," in *Hard x-ray and gamma-ray detector physics and applications*, *Proc. SPIE* **3446**, p. 218, 1998.
7. P. Chevart, U. El-Hanany, D. Schneider, and R. Triboulet, "CdTe and CdZnTe crystal growth by horizontal Bridgman technique," *J. Crystal Growth* **101**, p. 270, 1990.

8. T. Narita, P. F. Bloser, J. E. Grindlay, J. A. Jenkins, and H. W. Yao, "Development of IMARAD CZT detectors with PIN contacts," *Proc. SPIE* **3768**, 1999.
9. P. Bloser, J. Grindlay, T. Narita, and F. Harrison, "CdZnTe background measurement at balloon altitudes with an active BGO shield," in *EUV, X-ray, and Gamma-ray Instrumentation for Astronomy*, O. H. W. Siegmund and M. Gummin, eds., *Proc. SPIE* **3445**, p. 186, 1998.
10. T. W. Armstrong, B. L. Colborn, and B. D. Ramsey, "Initial estimates of radiation backgrounds in the cadmium-zinc-telluride focal plane detectors," *Science Applications International Corporation Report SAIC-TN-99015R*, 1999.
11. A. Parsons, S. Barthelmy, L. Bartlett, F. Birsa, N. Gehrels, J. Naya, J. Odom, S. Singh, C. Stahle, J. Tueller, and B. Teegarden, "CdZnTe background measurements at balloon altitudes," *Proc. SPIE* **2806**, p. 432, 1996.
12. K. Slavis, P. Dowkontt, F. Duttweiler, J. Epstein, P. Hink, G. Huszar, P. Leblanc, J. Matteson, R. Skelton, and E. Stephan, "High altitude balloon flight of CdZnTe detectors for high energy x-ray astronomy," in *EUV, X-ray, and Gamma-ray Instrumentation for Astronomy*, O. H. W. Siegmund and M. Gummin, eds., *Proc. SPIE* **3445**, p. 169, 1998.
13. K. R. Slavis, P. F. Dowkontt, J. W. Epstein, P. L. Hink, J. L. Matteson, F. Duttweiler, G. L. Huszar, P. C. Leblanc, R. T. Skelton, and E. A. Stephan, "Background studies in CZT detectors at balloon altitudes," *American Astronomical Society Meeting* **193**, pp. 6605+, Dec. 1998.